ELSEVIER

Polymer 42 (2000) 5471–5477

polymer

www.elsevier.nl/locate/polymer

Crystal ordering of α phase isotactic polypropylene

M. Naiki[a,*], T. Kikkawa[b], Y. Endo[b], K. Nozaki[b], T. Yamamoto[b], T. Hara[b]

[a]*Ube Research Laboratory, Ube Industries Ltd, Nishihon-machi, Ube 755-8633, Japan*
[b]*Department of Physics, Faculty of Science, Yamaguchi University, Yamaguchi 753-8512, Japan*

Received 19 July 2000; received in revised form 12 October 2000; accepted 13 November 2000

Abstract

Structural ordering from the α1 to the α2 phase of isotactic polypropylene has been investigated. The DSC studies showed that reorganization or recrystallization occurred in the wide endothermic region. In the high-temperature X-ray experiment of the sample annealed at 135°C, the $\bar{2}31$ and $\bar{1}61$ reflections ascribed to the α2 phase began to increase from 160°C and to decrease above 172°C. The *b*-axis length and the angle β of the unit cell increased up to 155°C and decreased afterward. The latter decrease was well correlated with an increase in the α2 phase. The α2 fraction increased in the temperature region where the degree of overall crystallinity decreased. Reorganization or recrystallization into the α2 phase is thus considered to occur with the fusion of the α1 phase, and the growth of the α2 phase in the solid state seems to be difficult.

Keywords: Isotactic polypropylene; α1–α2 transition; X-ray diffraction

1. Introduction

Molecular motions in semi-crystalline polymers at high temperatures are important subjects of research for understanding the structural ordering such as lamella thickening or melting processes [1]. In some polymer crystals the crystalline phase transitions are also induced on heating [2–5]. Molecular chains in crystals acquire mobility on heating; the conformational change, the rotation and diffusion of the molecular chains are likely to occur. These molecular motions in crystals, which are observed as a crystalline relaxation [6], are responsible for the physical properties at high temperatures.

Isotactic polypropylene (iPP) is the most fundamental stereoregular polymer and has been extensively investigated from academic and industrial interest. iPP can crystallize in three crystalline modifications and one mesomorphic form: monoclinic (α), hexagonal (β), orthorhombic (γ), and smectic [7,8]. The generation of these modifications can be controlled by crystallization conditions and molecular characters: for example, temperature, pressure, flow, nucleating agents, molecular weight and primary structure of molecular chains, etc. [7]. Although there are many crystalline phases in iPP, molecular chains form the 3_1 helical conformation in all crystalline phases and only the packing of molecular chains is different.

The structural changes in iPP on heating were found in the smectic, β and γ phases [9–11]; these phases are irreversibly transformed into the α phase which is stable at atmospheric pressure. The transformations have been examined by X-ray diffraction and DSC. The structural changes in the smectic and β phases have been considered to occur through melting and recrystallization into the α phase [9,10]. On the contrary, the solid state transition has been suggested in the γ phase [11], but it is still uncertain due to the peculiar unparalleled chain-packing [12,13].

There are two variants in the α phase: the less stable α1 phase (space group $C2/c$) [14] and the most stable α2 phase ($P2_1/c$) [15–17]. Both have a common arrangement of helical senses: on every (040) faces the winding direction of helices, left and right, is in alternate order. However, their methyl-group arrangement is different; in the α2 phase it is perfectly ordered while it is random in the α1 phase. It was clarified that the α iPP had various degrees of disorder in the up and down directions of the methyl groups [16,17], which means that usual iPP is a mixture of the α1 and the α2 phases. Hikosaka and Seto showed the phase transformation from the α1 to the α2 phase by annealing the former near the melting point [17]. The α1–α2 transition has become of interest relating to the double endotherms in the DSC heating thermgrams [18,19].

The change from the α1 to the α2 phase by annealing is

* Corresponding author. Tel.: +81-836-31-1703; fax: +81-836-31-2798.
E-mail address: 29418u@ube-ind.co.jp (M. Naiki).

0032-3861/017/$ - see front matter
PII: S0032-3861(00)00848-X

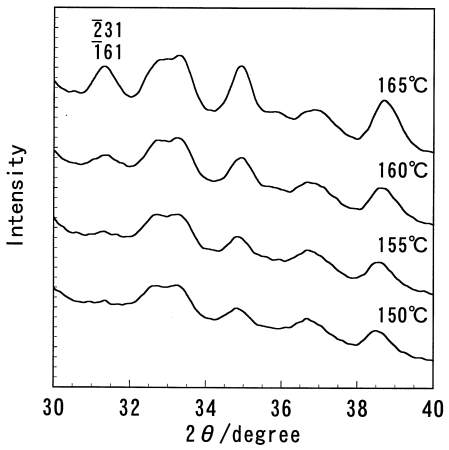

Fig. 1. X-ray diffraction profiles in the range of $2\theta = 30$–$40°$ of the annealed samples taken at room temperature. The samples were annealed at indicated temperatures for 2 h.

characterized by the rearrangement in methyl-group directions from a disordered state to an ordered one. Hikosaka and Seto explained that the α1–α2 transition occurred in solid state; they called the mechanism "order domain eduction model" that the domain of the α2 phase grew in the sea of the α1 phase[17]. On the other hand, Petraccone et al. concluded that this transition occurred through melting of the α1 phase followed by recrystallization into the α2 phase, from the fact that the variation in the order parameter of the up–down directions of the methyl groups corresponds with the beginning of the melting endotherm [18–20].

Though the transition from the α1 to the α2 phase has been discussed as mentioned above, the molecular mechanism has remained obscure. Thus far the structure of a sample after annealing has been examined by X-ray diffraction at room temperature and the details of the transition has not been clearly proven. In the present investigation, in order to clarify the mechanism of the transition from the α1 to the α2 phase, we examine not only the structure of a annealed sample at room temperature but also the structural change during the transition using X-ray diffraction at high temperatures. We demonstrate that the melting of the α1 crystal is deeply concerned in the α1–α2 transition.

2. Experimental

2.1. Material

The iPP used in this study was supplied by Grand Polymer, Ltd. The weight-averaged molecular weight and the molecular weight distribution determined by GPC were 290,000 and 4.8, respectively. The pentad isotacticity determined by ^{13}C NMR was 0.985. The atactic polypropylene was obtained as the *n*-hexane soluble fraction of an amorphous polypropylene, manufactured by Ube Industries Ltd, by Soxhlet extraction and was used for an amorphous material.

The iPP was melted and pressed into a sheet with 2 mm thickness at 200°C for 5 min to erase previous thermal history, and then quenched into an ice-water bath. The pressed sheet was annealed in an oil bath at various temperatures and time, and was quenched into a dry ice–methanol bath. The amorphous PP was also molded into sheet by compression molding.

2.2. Measurement

Thermal behavior was analyzed by a differential scanning calorimeter, Perkin–Elmer DSC7, which was calibrated by the melting of indium and *n*-heptane. Heating rates were 0.1–10°C min^{-1}.

X-ray diffraction was carried out using a MAC Science DIP220 imaging plate system. Graphite-monochromatized CuKα beam (40 kV, 250 mA) was transmitted through the sample. In a high-temperature X-ray experiment, the sample was held in the sample holder of a metal-block furnace. The temperature of the sample was measured by a thermocouple, which was contacted with the sample, and was controlled with a PID controller within ±0.1°C. After an X-ray diffraction pattern was measured by an exposure time for 10 min at the desired temperature, the sample was heated to the next temperature. This heating-measurement cycle was repeated until the sample melted.

The peak separation was made by a software of MAC Science imaging plate system. Curve fitting was made by a nonlinear least square method and the diffraction curve was separated into crystalline peaks and an amorphous halo. The scattering of the amorphous PP measured at various temperatures was used in resolving the amorphous contribution.

The appearance of the α2 phase was confirmed by the $\bar{2}31$ and $\bar{1}61$ reflections with $h + k =$ odd which are characteristically observed in the α2 phase (space group $P2_1/c$) and are absent in the α1 ($C2/c$) phase. The $\bar{2}31$ and $\bar{1}61$ reflections do not overlap with any other reflection. The fraction of the α2 phase was estimated by the method described in the literature [17,21].

3. Results

3.1. X-ray diffraction at room temperature

The appearance of the α2 phase greatly varies by the tacticity and the crystallization temperature of the sample used [21,22]. We should, therefore, first confirm the temperature at which the α2 phase is observed in our iPP sample prior to the examination of the crystalline structure at higher temperatures. We preliminarily took the diffraction patterns of the samples annealed at various temperatures below 165°C for 2 h. Diffraction profiles were obtained by scanning the imaging plate in the radial direction. Fig. 1 shows the profiles in the range of $2\theta = 30$–$40°$. At 155°C only a little $\bar{2}31$ and $\bar{1}61$ reflections at $2\theta = 31.6°$

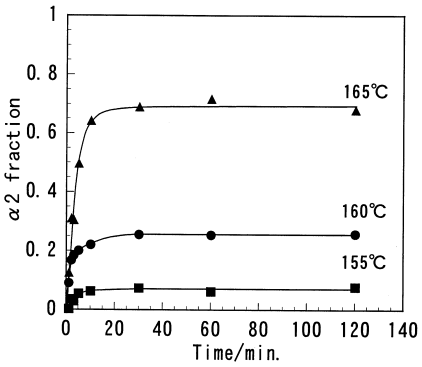

Fig. 2. The variation in the α2 fraction with time at 155°C (■), 160°C (●) and 165°C (▲).

characteristic of the α2 phase were observed, and above 160°C these reflections became definite. Though in a report by Hikosaka and Seto the α2 phase was observed from 125°C [17], these peaks were indistinguishable from noises even at 150°C, and we could not observe the α2 phase at such a low temperature.

The growth of the α2 phase with time at three different annealing temperatures is shown in Fig. 2. The samples were prepared by annealing for 1 min to 2 h followed by quenching into a dry ice–methanol bath. The fraction of the α2 rapidly increased with time at the beginning and became constant after a certain interval. The structural ordering almost terminated within the first 10 min; long time annealing has no effect on the α2 fraction. The transition occurs more readily as the annealing temperature increases.

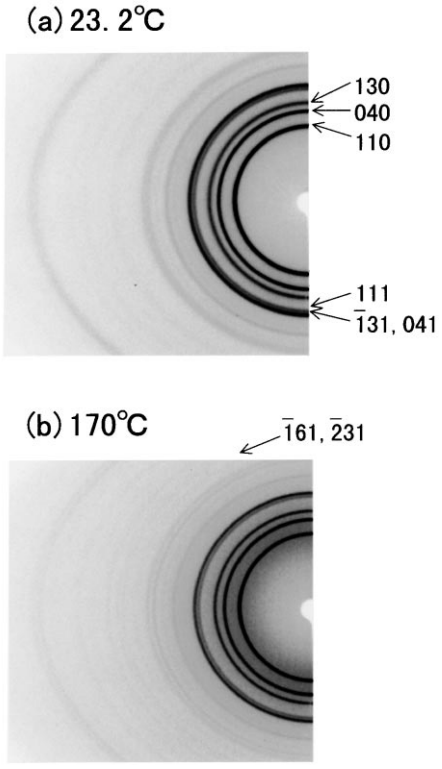

Fig. 3. X-ray diffraction patterns taken at (a) 23.2°C and (b) 170°C.

3.2. X-ray diffraction of α1 phase at high temperatures

It has been known that the heat treatment near the melting point induces the α1–α2 transition as shown in Fig. 1 [17–20]. However, the mechanism has not been clarified, since any structural change simultaneously occurring with the transition has not been examined. We investigate the change of the crystal structure of the α1 phase in stepwise heating from room temperature to the fusion. We used the sample annealed at 135°C for 2 h as a starting material. A series of X-ray diffraction patterns at various temperatures were collected.

The X-ray diffraction patterns at 23.2 and 170°C, which were both assigned to the α phase, are shown in Fig. 3. At 23.2°C, the width of the diffraction rings was large. At 170°C, when the intensity of the $\bar{2}$31 and $\bar{1}$61 reflections were maximum as it will be described later, the diffraction became sharp, but a strong amorphous halo was also observed. Furthermore, weak Bragg reflections appeared in the wider 2θ region. These show that the crystals became ordered but began to melt around 170°C. The reflections completely disappeared at 178°C. In the following, we precisely examine the process of the structural ordering by analyzing the X-ray diffraction patterns at each temperature.

Diffraction profiles were obtained over the whole area of the imaging plate. We first show the growth of the α2 phase on heating. Fig. 4 shows the X-ray diffraction profiles in the range of $2\theta = 30$–$40°$. The peaks were shifting to smaller angles due to thermal expansion of the crystal lattice. The intensity of reflections decreased due to the temperature factor when the sample was heated from room temperature to 135°C. The broad peak at $2\theta = 33°$ were well resolved into two peaks at higher temperatures. The most significant was that the $\bar{2}$31 and $\bar{1}$61 reflections in the vicinity of $2\theta = 31.2°$ appeared above 160°C and grew with increasing temperature. The intensity of these reflections reached a maximum at 170°C and decreased above 172°C. The increase in the intensity of the other peaks in Fig. 4 also come from the reflections with $h + k =$ odd, which overlap the reflections with $h + k =$ even.

Though, in Fig. 2, the intensity of the $\bar{2}$31 and $\bar{1}$61 reflections almost saturated in the sample annealed at 155°C within 10 min when it was measured at room temperature, these reflections were not observed on 10 min exposure at 155°C in Fig. 4. This is probably due to the difference in the thermal history; in Fig. 4, the sample was gradually annealed at lower temperature below 155°C resulting in the delay of the onset of melting, while in Fig. 1 the sample was directly annealed at 155°C without the experience of the lower temperature and partially melted at 155°C as shown later in DSC (Fig. 9).

We quantitatively analyzed the diffraction profiles at all temperatures; the lattice dimension and the degree of

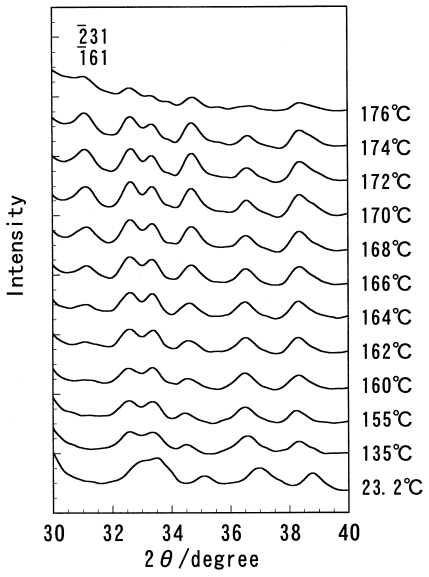

Fig. 4. Temperature dependence of X-ray diffraction profiles in the range of $2\theta = 30$–$40°$. The $\bar{2}31$ and $\bar{1}61$ reflections are developed above 160°C.

crystallinity were examined from the profiles. The curve at 164°C and the resolved peaks are shown in Fig. 5 as an example. The degree of apparent crystallinity, X_c, was obtained as a fraction of crystalline components in the 2θ range between 7 and 32°,

$$X_c = \frac{I_c}{I_c + I_a} \times 100 \quad (1)$$

where I_c and I_a are the sum of the area of the crystalline peaks and the area of the amorphous halo, respectively. The variation in the X_c is given in Fig. 6. The X_c gradually decreased with increasing temperature up to 150°C. This will be due to the fact that the diffraction intensity decreased by the thermal motion of the crystalline atoms and the resulting thermal diffuse scattering was counted as an amorphous scattering. The curve of X_c has a shoulder in the region of 155–164°C, where the structural ordering is comparable with the decrease in the diffraction intensity by the thermal motion of the atoms. Above 164°C the X_c decreased further, and the sample began to melt.

Fig. 7 shows the variation in the lattice constants during

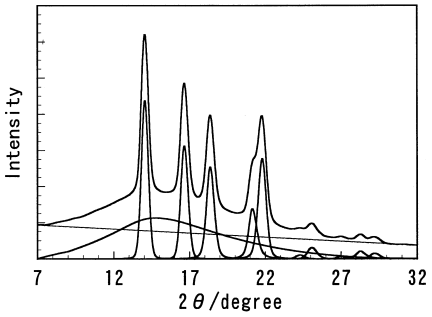

Fig. 5. X-ray diffraction profiles at 164°C and its peak resolution.

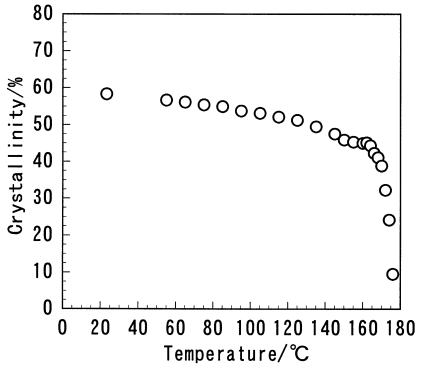

Fig. 6. Temperature dependence of the degree of crystallinity.

the temperature increase to 170°C followed by the decrease to room temperature. The *a*-axis and the *c*-axis lengths slightly varied with increasing temperature, while the variation in the *b*-axis is considerably larger than those in the other axes. This means that the *b*-axis is more sensitive to temperature change than the other axes. Moreover, the tendency of the variation in the *b*-axis length and the angle β was reversed at 155°C. On heating, crystallization was promoted by annealing and the crystalline lattice became contracted in the *b*-axis direction after it once thermally expanded. On the other hand, the *a*-axis and the *c*-axis lengths were monotonically increased and decreased, respectively, with increasing temperature.

In the cooling run in Fig. 7, the *b*-axis length and the angle β were irreversibly decreased to values smaller than the initial ones at room temperature. The *a*-axis and the *c*-axis lengths were reversibly decreased and increased, respectively. In the cooling process the crystals contracted in both the *a*-axis and the *b*-axis directions as the crystalline

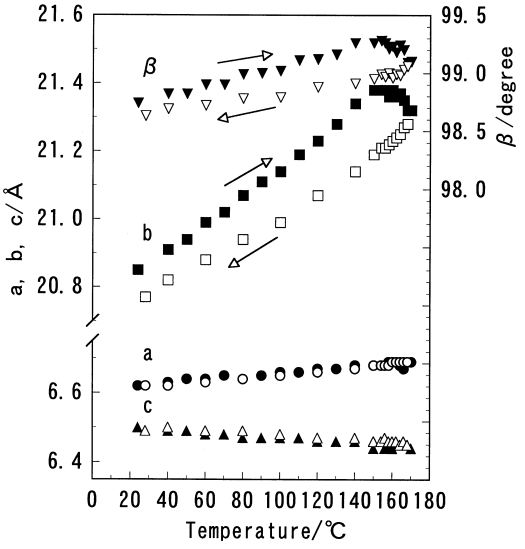

Fig. 7. The variations of the lattice parameters with temperature for the sample annealed at 135°C; heating run (closed symbols) and cooling run (open symbols).

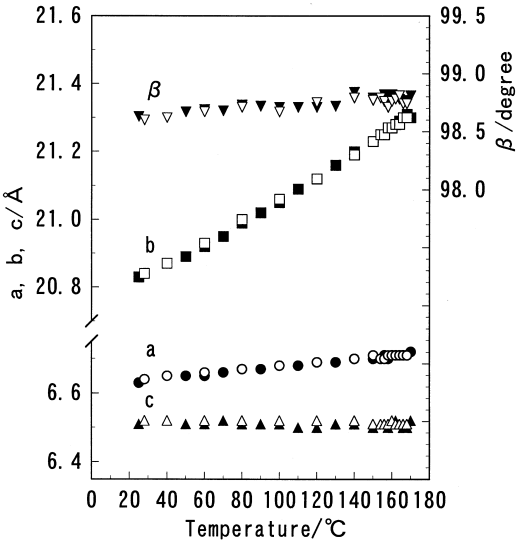

Fig. 8. The variations of the lattice parameters with temperature for the sample annealed at 170°C for 10 h; heating run (closed symbols) and cooling run (open symbols).

structure got more ordered. Since the variation in the *c*-axis length was small, the molecular chains are considered to retain 3_1 helical conformation in the heating and cooling cycle.

3.3. X-ray diffraction of the α2 phase at high temperatures

We show here the result of X-ray diffraction for the sample well annealed at a temperature high enough to be transformed into the α2 phase. The quenched sample was gradually heated to 170°C and was annealed at this temperature for 10 h resulting in the fully α2 phase sample. Fig. 8 shows the variations of the lattice parameters in the heating and cooling runs. All the parameters show reversible changes here, which are in contrast with the sample annealed at 135°C (α1, Fig. 7). Since the crystal was in the α2 phase from the beginning, only thermal expansion was observed. The expansion in the *b*-axis direction is again quite larger than those in the other directions. The overall thermal expansion in the α2 phase is smaller than that in the α1 phase [23].

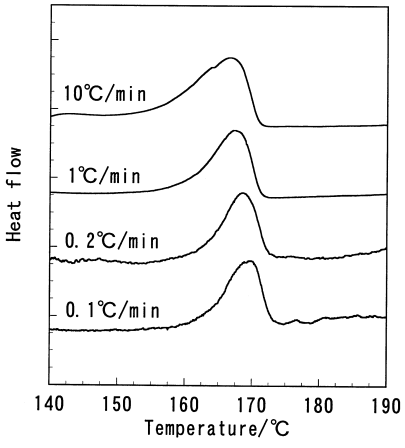

Fig. 9. DSC heating curves of the sample annealed at 135°C. Heating rates were varied between 0.1 and 10°C min^{-1}.

3.4. DSC

Fig. 9 shows DSC thermograms for iPP annealed at 135°C at different heating rates. Heating rates were varied between 0.1 and 10°C min^{-1}. Only one broad endotherm was observed. The endothermic peak shifted to higher temperature, when the heating rate was lowered. This indicates that the lamella thickening occurred through reorganization or recrystallization during heating. At a lower heating rate, there is more sufficient time for a component, once melted, to reorganize. The exothermic heat flow by reorganization or recrystallization was not observed probably because it was superposed on the endotherm.

It is impossible to compare exactly the X-ray experiment, which was carried out by keeping at the temperature of measurement for 10 min, with that of DSC of a constant heating rate. We have devised a DSC experiment, at the heating rate of 1°C min^{-1}, during the course of which the sample was kept at constant temperature for 10 min (Fig. 10). The holding temperatures are indicated in the figure. The endothermic peak temperature increased steadily with increasing holding temperature. This result also shows that reorganization or recrystallization occurs in the endothermic temperature range.

4. Discussion

4.1. DSC

The shape of the endotherm is affected by thermal and mechanical history. iPP often exhibits two endothermic peaks in the DSC heating run [18,19,24–26]. The two endothermic peaks have been attributed to melting and subsequent recrystallization; the second peak has been considered to represent the melting of a recystallized material. Petraccone et al. ingeniously reproduced double peaks by annealing iPP above 160°C and confirmed the α2 phase in the annealed samples [18,19]. From these results, they presumed that the double peaks of iPP near the α1 phase are concerned with the α1–α2 transition [18,19]. In our DSC studies, only one endothermic peak was observed at any of the heating rates (Fig. 9). Our samples were prepared by annealing at 135°C. The difference in the number of endothermic peaks, single or double, arises from the difference in the thermal history of the sample used; Petraccone et al. annealed them above 160°C and we at 135°C. Regardless of the number of the endothermic peaks, the reorganization or the α1–α2 transition occurs in the wide endothermic temperature region.

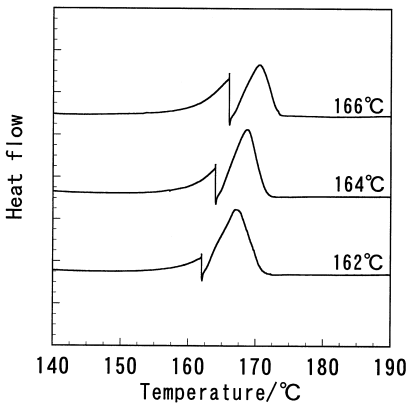

Fig. 10. DSC heating curves at 1°C min^{-1}. Heating was interrupted at the indicated temperatures for 10 min.

4.2. Crystal ordering at high temperatures

The X-ray experiments indicated that the crystal structure became ordered by heat treatments at high temperatures. The temperature dependence of the *b*-axis length and the angle β of the α1 phase was correlated with each other; they gradually increased in the temperature range up to 155°C and decreased afterward (Fig. 7). In the α2 phase no contraction was observed in the heating run (Fig. 8). On the other hand, the variation in the *a*-axis was a monotonic increase. The contraction in the *b*-axis and the angle β in the heating run is correlated with the growth of the α2 phase very well. This denotes that the transition reveals in the lattice dimension. The molecule came to pack densely in the *b*-axis direction with ordering into the α2 phase. That is to say, the distance between chains in the *b*-axis direction in the α2 phase is closer than that in the α1. The variation in the lattice constants shows that the *b*-axis is more sensitive to thermal expansion and the structural change than the *a*-axis.

The temperature dependence of the α1 and the α2 fractions is plotted in Fig. 11 where the data are compared with the apparent crystallinity, X_c. The decrease and increase in the α1 and α2 fractions, respectively, clearly demonstrate the transformation of the α1 into the α2 phase. In the range

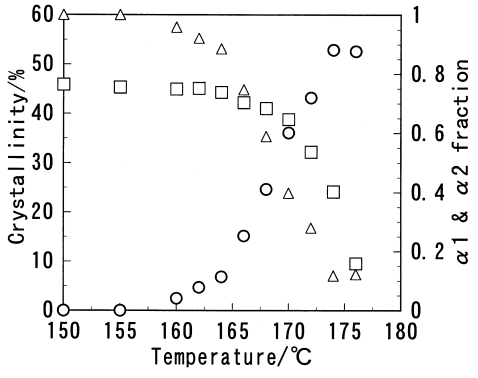

Fig. 11. Comparison of the crystallinity (□), the α1 (△) and the α2 fraction (○).

of 155–164°C where X_c was constant, the decrease in the diffraction intensity by thermal motions is balanced with the increase in the degree of crystallinity. Therefore, at the temperature where the $\bar{2}31$ and $\bar{1}61$ reflections began to be observed, reorganization or recrystallization occurred. Above 164°C, the fusion was considered more abundant than ordering, because X_c decreased.

The α2 phase appeared at 160°C and its fraction increased even above 164°C where the apparent crystallinity decreased. This may be a strange behavior since the particular peaks characteristic of the α2 phase grow while the others decrease by melting. This strongly suggests that the α2 phase grows after the α1 phase once melts. From the results of DSC experiments shown in Figs. 9 and 10, it is considered that the reorganization or recrystallization occurred in the wide endothermic region. The crystalline modification transformed to the α2 phase in the endothermic region, as we confirmed by X-ray diffraction. Therefore, it is reasonable to consider that the α2 phase grows through the melting-reorganization or melting-recrystallization mechanism.

In the samples annealed in an oil bath, the α2 phase was observed at a lower temperature of 155°C (Fig. 1). In the DSC thermogram at a heating rate of 10°C min^{-1}, a little exotherm already began at 155°C (Fig. 9). The sample partially melted at 155°C by rapid heating in the oil bath and the melting portion recrystallized into the α2 phase.

If the α1–α2 transition occurred in the solid state, it might be thought that the more stable α2 phase would gradually increase with time. However, the time dependence of the α2 growth during annealing shows that the α2 fraction increases at the initial stage of annealing and becomes constant even if the sample is retained at high temperatures for a long time (Fig. 2). Only a movable or melting portion at the temperature can transform into the α2 phase, and no more α2 phase increases by slow rearrangements of the molecular chains. This suggests that the exchange of molecular chains in a solid state is very difficult.

Finally we consider here the α1–α2 transition in the solid state. When the conformational change of the iPP molecule is considered, it is impossible to independently reverse the winding direction: right (R) and left (L) and the direction of the methyl group: up and down. A helical chain can change between R–up and L–down or between L–up and R–down [27]. The structural change from the α1 to the α2 phase is known to be described as the ordering of the direction of the methyl groups. If the α1 phase is transformed into the α2 phase through the inversion of the direction of the methyl groups, it is necessary that the molecular chains replace their positions because the inversion of the methyl groups causes the inversion of the winding direction; rewound chains cannot occupy their original positions in the lattice. According to our simulation in the solid state, the α2 phase can grow in the α1 matrix only when the exchange of the neighboring molecules are allowed [28]. However, it seems difficult that the long stems with bulky methyl groups

replace each other in the solid state, even if crystals thermally expand. Actually, the α2 phase will greatly grow while the α1 phase partially melts.

5. Conclusions

We investigated the structural ordering in iPP at high temperatures by X-ray diffraction and DSC, and especially examined the α1–α2 transition. In the high temperature X-ray experiment, the $\bar{2}31$ and $\bar{1}61$ reflections characteristic of the α2 phase appeared above 160°C. The lattice contraction in the *b*-axis direction and in the angle β above 155°C well correlated with an increase in the α2 phase. On the other hand, the *a*-axis and *c*-axis lengths monotonically increased. At the temperature where the $\bar{2}31$ and $\bar{1}61$ reflections began to be observed, the increase in the crystallinity was balanced by the decrease in the diffraction intensity by thermal motion of atoms. The intensity of these reflections increased even above 164°C where the degree of crystallinity decreased; the α2 phase grew while the α1 phase melted. The DSC showed that the reorganization or recrystallization occurred in the wide endothermic region. Further, molecular rearrangement in the solid state is considered to be hard to occur. From these results, we conclude that the α2 phase grows through the melting of the α1 phase followed by reorganization or recrystallization into the α2 phase.

Acknowledgements

We wish to thank T. Akagawa of Grand Polymer, Ltd, for kindly providing the iPP samples.

References

[1] Bassett DC. Principles of polymer morphology. Cambridge: Cambridge University Press, 1981 (chap. 5).
[2] Yamamoto T, Hara T. Polymer 1982;23:521–8.
[3] Tashiro K, Sasaki S, Kobayashi M. Macromolecules 1996;29:7460–9.
[4] Colclough ML, Baker R. J Mater Sci 1978;13:2531–40.
[5] Tashiro K, Kobayashi M. Phase Transitions 1989;18:213–46.
[6] Kawai H, Hashimoto T, Suehiro S, Fujita K. Polym Engng Sci 1984;24:361–72.
[7] Brückner S, Meille SV, Petraccone V, Pirozzi B. Prog Polym Sci 1991;16:361–404.
[8] Cheng SZD, Janimak JJ, Rodriguez J. In: Karger-Kocsis J, editor. Polypropylene: structure, blends and composites, vol. 1. London: Chapman and Hall, 1995 (chap. 2).
[9] Alberola N, Fugier M, Petit D, Fillon B. J Mater Sci 1995;30:1187–95.
[10] Vleeshouwers S. Polymer 1997;38:3213–21.
[11] Karods JL, Cristiansen AW, Baer E. J Polym Sci: A-2 1966;4:777–88.
[12] Brückner S, Meille SV. Nature 1989;340:455–7.
[13] Meille SV, Brückner S, Porzio W. Macromolecules 1990;23:4114–21.
[14] Natta G, Corradini P. Nuvo Cimento Suppl 1960;15:40–51.
[15] Mencik Z. Chem Prum 1960;10:377–81.
[16] Mencik Z. J Macromol Sci Phys 1972;B6:101–15.
[17] Hikosaka M, Seto T. Polym J 1973;5:111–27.
[18] De Rosa C, Guerra G, Napolitano R, Petraccone V, Pirozzi B. Eur Polym J 1984;20:937–41.
[19] Guerra G, Petraccone V, Corradini P, De Rosa C, Napolitano R, Pirozzi B, Giunchi G. J Polym Sci: Polym Phys 1984;22:1029–39.
[20] Corradini P, Giunchi G, Petraccone V, Pirozzi B, Vidal HM. Gazz Chim Ital 1980;110:413–8.
[21] Radhakrishnan J, Ichikawa K, Yamada K, Toda A, Hikosaka M. Polymer 1998;39:2995–7.
[22] Naiki M, Fukui Y, Matsumura T, Nomura T, Matsuda M. Kobunshi Ronbunshu 1998;55:512–8.
[23] Napolitano R, Pirozzi B, Varriale V. J Polym Sci: Polym Phys 1990;28:139–47.
[24] Petraccone V, Guerra G, De Rosa C, Tuzi A. Macromolecules 1985;18:813–4.
[25] Yadav YS, Jain PC. Polymer 1986;27:721–7.
[26] Alamo RG, Brown GM, Mandelkern L, Lehtinen A, Paukkeri R. Polymer 1999;40:3933–44.
[27] Tadokoro H. Structure of Crystalline Polymers. New York: Wiley, 1979 (chap. 7).
[28] Hirose M, Yamamoto T, Naiki M. Comput Theor Polym Sci 2000;10:345–53.